

gle crystals of MnF_2 . It is a pleasure to thank Dr. D. Gill, Dr. J. Jeener, and Dr. G. Seidel for many helpful discussions.

*Research supported by the U. S. Joint Services and Advanced Research Projects Agency.

†Raytheon Predoctoral Fellow 1959-60; Texaco Predoctoral Fellow 1960-61; now at Massachusetts Institute of Technology, Cambridge, Massachusetts.

¹R. G. Shulman and V. Jaccarino, Phys. Rev. 108, 1219 (1957).

²V. Jaccarino and R. G. Shulman, Phys. Rev. 107,

1196 (1957).

³G. T. Armstrong, J. Research Natl. Bur. Standards 53, 263 (1954).

⁴G. B. Benedek and T. Kushida, Phys. Rev. 118, 46 (1960).

⁵N. J. Poulis and G. E. G. Hardeman, Physica 18, 391 (1952).

⁶V. Jaccarino and L. R. Walker, J. phys. radium 20, 341 (1959).

⁷J. W. Stout and M. Griffel, J. Chem. Phys. 18, 1455 (1950).

⁸T. Moriya, Progr. Theoret. Phys. (Kyoto) 16, 641 (1956).

⁹D. F. Gibbons, Phys. Rev. 115, 1194 (1959).

MICROWAVE GENERATION IN RUBY DUE TO POPULATION INVERSION PRODUCED BY OPTICAL ABSORPTION*

D. P. Devor, I. J. D'Haenens, and C. K. Asawa
Hughes Research Laboratories, Malibu, California

(Received April 30, 1962)

Microwave amplification and generation by the stimulated emission of radiation (maser) were observed in ruby as a result of population inversion produced in the ground state of Cr^{3+} by the absorption of the coherent optical emission from a second ruby (optical maser). The maser crystal was oriented in a magnetic field of about 6700

Oe to obtain a transition between a ground 4A_2 Zeeman sublevel and an excited $\bar{E}(^2E)$ Zeeman sublevel which would match a spectral component of the output of the optical maser. The arrangement of the experimental apparatus is shown schematically in Fig. 1.

Detection of the interaction of optical and para-

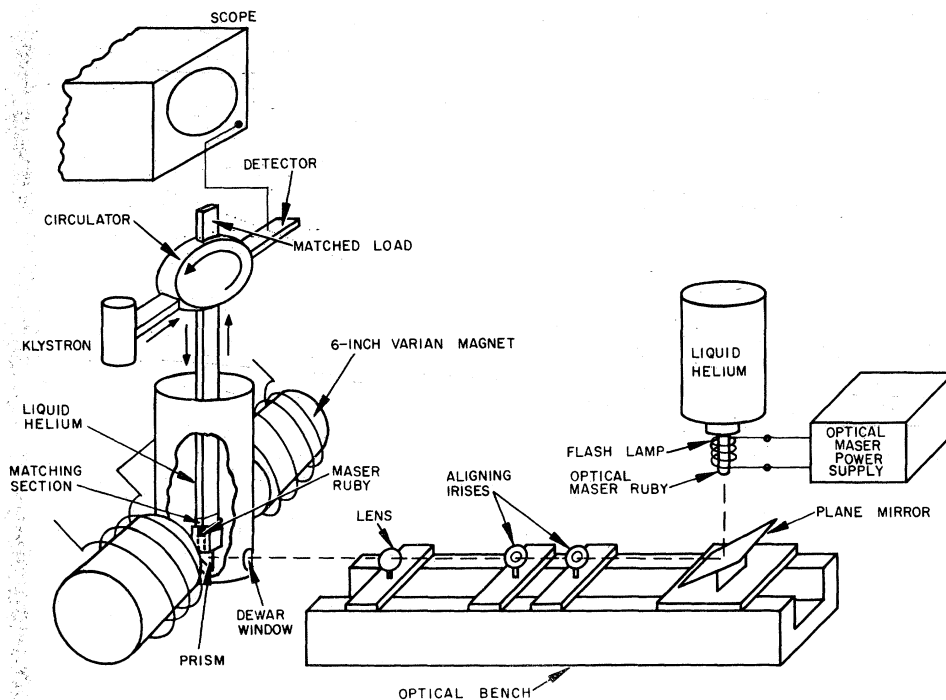


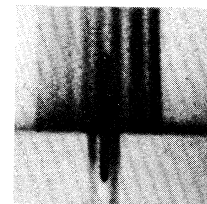
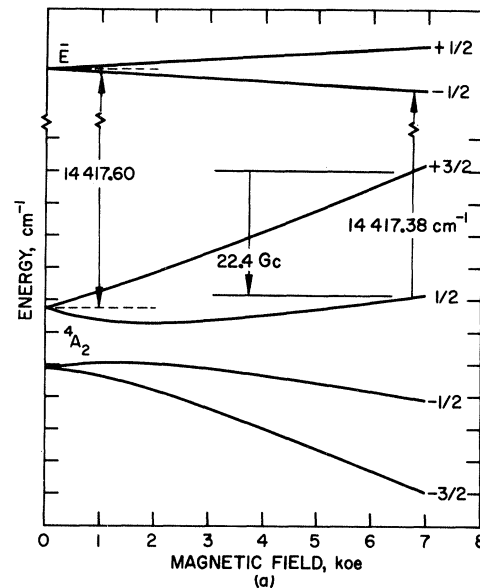
FIG. 1. Arrangement of experimental apparatus.

magnetic transitions in the sharp line spectra of ions in crystalline solids has been accomplished previously through the observation of the effect of the paramagnetism on the optical signals.¹⁻³ Wieder¹ attempted to directly detect the effect on paramagnetism of depopulation in the 4A_2 state in ruby due to the absorption of the *R*-line fluorescent light. Since the optical spectrum of the ruby optical maser results from *R*-line emission, the optical maser offered a considerably better optical source (in terms of collimation, spectral purity, and power output) for such an experiment, not only to detect perturbation of the ground-state populations, but also to produce population inversion.

D'Haenens and Asawa⁴ have observed stimulated optical emission in ruby to shift to longer wavelengths from the fluorescent emission. In the present experiment, the optical-maser crystal, initially cooled by conduction to liquid-helium temperature, produced a pump signal of 6934.188 Å (air wavelength) from the $\bar{E}({}^2E) \rightarrow \pm \frac{1}{2}({}^4A_2)$ transition (spin states correspond to high-field assignments). The optical-maser output was unpolarized.

The separation of the $\bar{E}({}^2E)$ and the $\pm \frac{1}{2}({}^4A_2)$ states in the maser crystal was taken as the fluorescent wavelength of 6934.082 Å at 4.2°K. The *g* value of the \bar{E} Kramers' doublet was obtained from the work of Geschwind, Collins, and Schawlow,² and the Zeeman structure of the 4A_2 ground state was known from the analysis of Chang and Siegman.⁵ From their data we calculated that the magnetic field at an angle of 67 degrees, with respect to the crystalline *c* axis, split the \bar{E} and 4A_2 states as shown in Fig. 2(a). At 6700 Oe, the $+\frac{1}{2}(\bar{E}) \rightarrow +\frac{1}{2}({}^4A_2)$ transition matched the $\bar{E} \rightarrow \pm \frac{1}{2}({}^4A_2)$ component of the optical-maser spectrum, since the latter transition was 0.22 cm^{-1} less than the fluorescent wave number in zero field. The $+\frac{3}{2}({}^4A_2) \rightarrow +\frac{1}{2}({}^4A_2)$ microwave transition occurred at 22.4 Gc/sec. Figure 2(b) shows a comparison of the fluorescence and optical-maser emission spectra under approximately such conditions. The spectral agreement of the $-\frac{1}{2}(\bar{E}) \rightarrow +\frac{1}{2}({}^4A_2)$ transition in fluorescence with the lower energy optical-maser line indicated that the magnitude and orientation of the magnetic field were not particularly critical.

The microwave resonant structure consisted of a section of 0.050- by 0.130-inch waveguide which was beyond cutoff at 22.4 Gc/sec and was partially loaded with a 0.078-inch length of ruby. The structure acted as a ruby-loaded microwave



WAVELENGTH λ INCREASING \rightarrow
(b)

FIG. 2. Comparison of the spectra of ruby in fluorescence and in stimulated emission under conditions suitable for optical pumping. (a) Zeeman structure of Cr^{3+} ruby. The crystalline *c* axis is oriented at 67 degrees with respect to the magnetic field. The *g* factor of the \bar{E} state is 0.956, as given by Geschwind et al.² (b) Comparison of spectrographs of ruby in fluorescence (upper eight lines) and in stimulated emission at a temperature of 4.2°K. The fluorescence was observed with the *c* axis at 70 degrees with respect to a magnetic field of 6500 Oe. The short line is the neon reference in ninth order corresponding to $\lambda = 6934.0831$ Å. Spectra were taken with a special Harrison grating.

reflection cavity resonant at 22.4 Gc/sec in a perturbed TE_{011} mode. At liquid-nitrogen temperature, the quality factor Q_0 of this structure, exclusive of magnetic losses and external circuit losses, was about 1600. The filling factor was calculated to be 96%.

The conditions for power gain and/or oscillation in a solid-state maser are given by Bloembergen⁶ in terms of the magnetic quality factor Q_m . To overcome the microwave circuit losses,

the quality factor Q_0 of the structure must exceed $|Q_m|$ when population inversion is obtained. The population of the \bar{E} state is extremely small at 4.2°K and, consequently, saturation of the $+\frac{1}{2}(^4A_2) \rightarrow -\frac{1}{2}(\bar{E})$ pump transition depletes the $+\frac{1}{2}(^4A_2)$ state of one-half the Boltzmann population. The maser crystal was cut from 0.05 wt.% $\text{Cr}_2\text{O}_3:\text{Al}_2\text{O}_3$ ruby, giving a Boltzmann population of 3.06×10^{16} in the $+\frac{1}{2}(^4A_2)$ level. Thus, the absorption of 1.53×10^{16} photons, or 4.39×10^{-3} joule of pump signal, is required for saturation of the $+\frac{1}{2}(^4A_2) \rightarrow -\frac{1}{2}(\bar{E})$ transition; this amount of energy is orders of magnitude less than that available from the optical maser. Using appropriate data for ruby and the present microwave cavity, the magnetic Q obtained from the saturation of the $+\frac{1}{2}(^4A_2) \rightarrow -\frac{1}{2}(\bar{E})$ transition is $-Q_m \cong 75$, which is considerably less than the Q_0 of the microwave resonant structure.

The experimental results are shown in Fig. 3. The klystron signal generator was frequency modulated at a repetition rate which allowed us to sample the relative populations of the 4A_2 sub-levels while the microwave system was being optically pumped. This low effective duty cycle was chosen to avoid microwave saturation effects. The cavity was undercoupled in the absence of paramagnetic resonance. The traces in Fig. 3(a) are recordings of the optical-maser output and a 200- μsec -delayed display of the microwave reflected power. The first klystron sweep shows the ruby sample absorbing at the $+\frac{1}{2}(^4A_2) \rightarrow +\frac{3}{2}(^4A_2)$ transition; the second sweep shows the reduction in magnetic losses as $1/Q_m$ goes to zero (or becomes slightly negative) due to depopulation of the $+\frac{1}{2}(^4A_2)$ level; on the third sweep, $1/Q_m$ is sufficiently negative to produce amplification.

In Fig. 3(b) the microwave coupling to the maser crystal was reduced, the optical-maser output was increased, and the klystron power level was the same as that in Fig. 3(a). Figure 3(b) shows simultaneous amplification and oscillation. For the trace in Fig. 3(c) the klystron was turned off and oscillation was produced. The pulsed nature of the oscillation was the same as that observed in microwave-pumped ruby masers by Makhov *et al.*⁷ and Foner *et al.*⁸ The $-\frac{1}{2}(^4A_2) \rightarrow +\frac{1}{2}(^4A_2)$ resonance was observed with a small increase in magnetic field. A re-recording of this resonance, when the optical maser illuminated the maser crystal, showed that the microwave absorption increased markedly [Fig. 3(d)] and thus confirmed the pumping of the

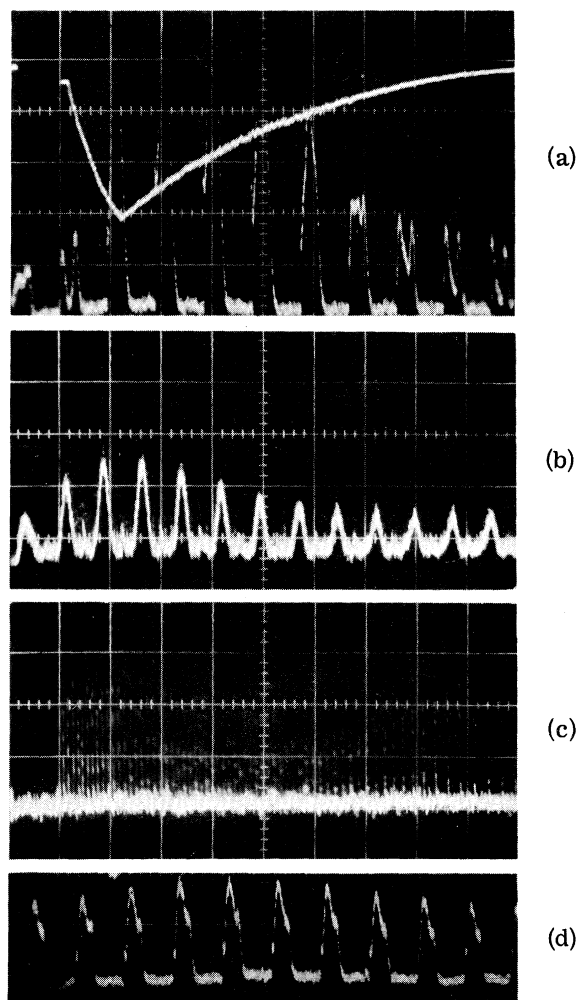


FIG. 3. Experimental results. (a) Optical-maser output and a 200- μsec -delayed signal of reflected microwave power from the microwave cavity showing amplification at 22.4 Gc/sec. The optical-maser output was about 2.5 joules of which 1 joule was estimated to be incident on the maser crystal. Time scale = 200 μsec /division; input microwave power level $\approx 50 \mu\text{W}$. (b) Simultaneous maser oscillation and amplification. Conditions as in (a) except microwave coupling to the maser crystal was reduced; also, the optical-maser output was increased to about 4 joules of which about 2.8 joules were estimated to be incident on the maser crystal. (c) Maser oscillation observed with no input microwave signal. Time scale = 50 μsec /division. (d) Increased microwave absorption at the $-\frac{1}{2}(^4A_2) \rightarrow +\frac{1}{2}(^4A_2)$ transition due to depopulation of the $+\frac{1}{2}(^4A_2)$ level. All conditions were as in (a).

$+\frac{1}{2}(^4A_2)$ level.

The microwave structure appeared to have two resonant modes separated by 30 or 40 Mc/sec, possibly as a result of the anisotropy

of the dielectric constant of sapphire and a slight misalignment of the crystalline c axis from the rectangular axis of the cut crystal. The maser was occasionally observed to amplify in both modes simultaneously, although not with equal gain.

With the technique described here, amplification and oscillation at frequencies considerably higher than 22.4 Gc/sec are possible; thus, a brief examination of the energy levels of ruby indicates that amplification at 57 Gc/sec in a magnetic field of 21 000 Oe could be obtained. In addition, the excited state can be selectively populated to allow direct observation of paramagnetic resonance in this state. Furthermore, maser gain was observed for some time after the loss of the liquid helium in the maser Dewar, thus indicating the possibility of operating at temperatures higher than 4.2°K.

The efficacy of the optical maser in an optical-pumping experiment was, to our knowledge, first

considered by T. H. Maiman and R. H. Hoskins. Considerable help with the microwave resonant structure was obtained from J. E. Keifer and F. E. Goodwin.

*Work supported by the U. S. Army Signal Corps under Contract DA 36-039 SC-87221.

¹Irwin Weider, Phys. Rev. Letters 3, 468 (1959).

²S. Geschwind, R. J. Collins, and A. L. Schawlow, Phys. Rev. Letters 3, 545 (1959).

³J. Brosnel, S. Geschwind, and A. L. Schawlow, Phys. Rev. Letters 3, 548 (1959).

⁴I. J. D'Haenens and C. K. Asawa (to be published).

⁵W. S. Chang and A. E. Siegman, Stanford Electronic Laboratory, Technical Report No. 156-2, Stanford University, California (unpublished); also as reproduced by J. Weber, Revs. Modern Phys. 31, 681 (1959).

⁶N. Bloembergen, Phys. Rev. 104, 324 (1956).

⁷G. Makhov, C. Kikuchi, J. Lamb, and R. W. Terhune, Phys. Rev. 109, 1399 (1958).

⁸S. Foner, L. R. Momo, and A. Mayer, Phys. Rev. Letters 3, 36 (1959).

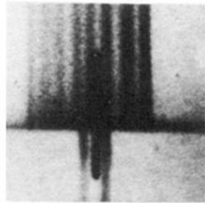
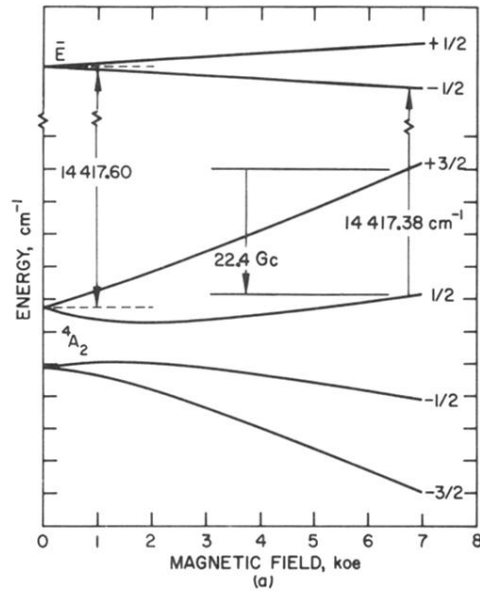


FIG. 2. Comparison of the spectra of ruby in fluorescence and in stimulated emission under conditions suitable for optical pumping. (a) Zeeman structure of Cr^{3+} ruby. The crystalline c axis is oriented at 67 degrees with respect to the magnetic field. The g factor of the \bar{E} state is 0.956, as given by Geschwind et al.² (b) Comparison of spectrographs of ruby in fluorescence (upper eight lines) and in stimulated emission at a temperature of 4.2°K. The fluorescence was observed with the c axis at 70 degrees with respect to a magnetic field of 6500 Oe. The short line is the neon reference in ninth order corresponding to $\lambda = 6934.0831 \text{ \AA}$. Spectra were taken with a special Harrison grating.

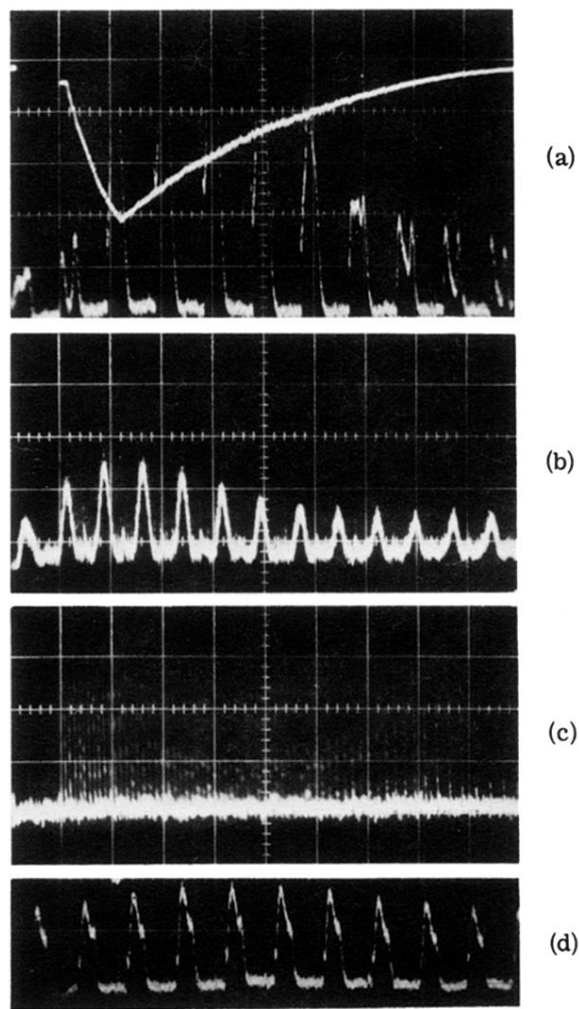


FIG. 3. Experimental results. (a) Optical-maser output and a 200- μ sec-delayed signal of reflected microwave power from the microwave cavity showing amplification at 22.4 Gc/sec. The optical-maser output was about 2.5 joules of which 1 joule was estimated to be incident on the maser crystal. Time scale = 200 μ sec/division; input microwave power level $\approx 50 \mu$ W. (b) Simultaneous maser oscillation and amplification. Conditions as in (a) except microwave coupling to the maser crystal was reduced; also, the optical-maser output was increased to about 4 joules of which about 2.8 joules were estimated to be incident on the maser crystal. (c) Maser oscillation observed with no input microwave signal. Time scale = 50 μ sec/division. (d) Increased microwave absorption at the $-\frac{1}{2}(^4A_2) \rightarrow +\frac{1}{2}(^4A_2)$ transition due to depopulation of the $+\frac{1}{2}(^4A_2)$ level. All conditions were as in (a).